Lawrence Berkeley National Laboratory
Recent Work

Title
MESON MASS MEASUREMENTS II ON THE MEASUREMENT OF MASSES OF CHARGED PIONS

Permalink
https://escholarship.org/uc/item/4pq753pv

Author
Smith, Frances M.

Publication Date
1954-02-02

eScholarship.org Powered by the California Digital Library
University of California

UCRL 2371

UNIVERSITY OF CALIFORNIA

Radiation Laboratory

TWO-WEEK LOAN COPY

This is a Library Circulating Copy
which may be borrowed for two weeks.
For a personal retention copy, call
Tech. Info. Division, Ext. 5545

BERKELEY, CALIFORNIA

DISCLAIMER

This document was prepared as an account of work sponsored by the United States Government. While this document is believed to contain correct information, neither the United States Government nor any agency thereof, nor the Regents of the University of California, nor any of their employees, makes any warranty, express or implied, or assumes any legal responsibility for the accuracy, completeness, or usefulness of any information, apparatus, product, or process disclosed, or represents that its use would not infringe privately owned rights. Reference herein to any specific commercial product, process, or service by its trade name, trademark, manufacturer, or otherwise, does not necessarily constitute or imply its endorsement, recommendation, or favoring by the United States Government or any agency thereof, or the Regents of the University of California. The views and opinions of authors expressed herein do not necessarily state or reflect those of the United States Government or any agency thereof or the Regents of the University of California.

UCRL-2371
Unclassified - Physics
Distribution

UNCLASSIFIED

UNIVERSITY OF CALIFORNIA
Radiation Laboratory

Contract No. W-7405-eng-48

MESON-MASS MEASUREMENTS II
ON THE MEASUREMENT OF THE MASSES OF CHARGED PIONS

Frances M. Smith

February 2, 1954

Berkeley, California

MESON-MASS MEASUREMENTS II
ON THE MEASUREMENT OF THE MASSES OF CHARGED PIONS

Table of Contents

UCRL-2371
Unclassified - Physics
Distribution

MESON-MASS MEASUREMENTS II
ON THE MEASUREMENT OF THE MASSES OF CHARGED PIONS

Frances M. Smith

Radiation Laboratory, Department of Physics,
University of California, Berkeley, California

February 2, 1954

ABSTRACT

This paper describes the method developed and the results obtained in an extensive program of measurement of the masses of charged pions. Measurements were made of the total ranges in nuclear track emulsion and the momenta (obtained from the curving of theparticle trajectory in the magnetic field of the 184-inch cyclotron) of pions and protons of nearly the same velocity. This procedure eliminates any strong dependence on a range-momentum relationship for determining particle mass ratios.

A beam of monoenergetic particles stopping in matter will have a distribution of ranges that is nearly Gaussian. Therefore the measurements in this study were treated statistically by introducing that function of the mass (the normalized range) which has a linear dependence on the range. The straggling theory was checked by examining the range distribution of monoenergetic muons. The distribution was found to be consistent with the theoretical expectations when allowance was made for several known sources of variance in addition to the so-called Bohr straggling. For a particle β of $\simeq 0.27$ the range straggling of muons in 200-micron C-2 emulsion is $(4.5 \pm 0.1)\%$, that of pions is $(4.0 \pm 0.1)\%$, and that of protons is $(1.2 \pm 0.1)\%$.

A dependence of the apparent mass on the variable stopping power of the emulsion was eliminated from the mass ratio by taking the ratio of the expectation value of the normalized range of positive pions to that of protons. The apparent mass ratio was corrected for the small effect of the finite sizes of target and detector and for the so-called Lewis effect. The mean value of M(the true mass ratio) as found from six plates was 0.14883 ± 0.00016.

In a second part of the study the ratio of the expectation value of the normalized range of negative pions to that of positive pions was found from three plates. The mean value of the true ratio of the mass ($\mathfrak{M}$) of the negative to that of the positive pion was 0.998 ± 0.002. This ratio has been corrected for the small difference in stopping cross section to be expected for particles of opposite sign.

MESON-MASS MEASUREMENTS II
ON THE MEASUREMENT OF THE MASSES OF CHARGED PIONS

Frances M. Smith

Radiation Laboratory, Department of Physics,
University of California, Berkeley, California

February 2, 1954

I. INTRODUCTION

The answer to the question, "What is the mass of the meson?", is of importance not only in the theories of nuclear forces but for its intrinsic interest. The attempts to find the answer have been numerous and have encompassed a diversity of methods of approach to the question. The kinds of information obtained from these investigations have added to the knowledge needed in establishing the validity of the theories of nuclear and atomic processes (for a précis of these studies see the introduction of Paper I* in this series). These studies have revealed the existence of different types of particles of intermediate mass.[1]

This study had its inception in 1948[2] when mesons, produced from target nuclei bombarded by the alpha-particle beam in the 184-inch synchrocyclotron, were first detected. Since that time there has been a series of experiments[3] for the purpose of measuring the masses of mesons. This paper presents only the final measurements in the series. The method used embodies all the refinements of technique and theory developed from the previous inquiries.

II. METHOD

A. The Range-Momentum Relation

The method used in this study is essentially that of calculation of the momenta of the particles by means of their magnetic rigidities (or $H\rho$'s) as determined in the strong field of the cyclotron, along with measurement of their total ranges in the material of the detector. The relationship between these two quantities and the mass of the particles of interest must be known for the particular detector. This method is commonly referred to as "The method of $H\rho$ and range."

The detector used in all these studies was 1-in. x 3-in. glass-backed nuclear track emulsion. Nuclear track emulsion is well suited to measurement of range as it performs the function of both absorber and detector. It provides visual

*UCRL-2327

evidence of the progress of the particle and thus allows an accurate determination of the total range. The fairly high stopping power permits absorption of particles of moderate incident energy within a relatively small distance.

The range-momentum relation is obtained for a particle of charge ze by use of the assumption that the space rate of energy loss is a function of the velocity alone. This leads directly to the expression: $z^2 R/M = f(p/M)$ R = range

p = momentum

M = rest mass

The range-momentum relation for protons in 200-micron Ilford C-2 emulsion has been determined for a comparatively wide range of proton energies. (For a critique of this determination refer to Paper I, Sec. IV.) The relation can be expressed: $z^2 R/M = c\,(p/M)^q$. This is an ideal relation. In practice one has to consider the effects of range straggling, the magnitude of the mass of the penetrating particle and the uncertainty of the momentum due to the finite source of the particle. It was found that over the small range of energies of the protons used in this study (kinetic energy $T \simeq 33.6$ Mev) $c \simeq 6.8 \times 10^{-21}$ and $q = 3.44$ for R in microns, p in gauss mm. and M in proton masses.

The q in the equation is a very slowly varying function and, as was indicated in Paper I, is constant over the energies used in this experiment. The value 3.44 ± 0.03 seems consisistent with all data. Furthermore the value of q is at a maximum in this region of energies, thus $dq/dT = 0$ (see Paper I, Sec. IV, B). The c is the constant for the emulsion used. Since the emulsion does not have an absolutely invariant composition (especially in water content) the "constant" c varies with batch and exposure conditions. In view of this variation a method that eliminates c was used to determine the mass of the pion. The most logical procedure was to expose the same film to pions and protons with equal velocities. If the velocities of the pion and proton are equal, the ratio of their respective ranges is equal to the ratio of their momenta and is also the ratio of their masses. The charge on the meson presumably is the same as that on the proton. Results of previous experiments seem to indicate that it is.[4] The velocities of the pions and protons were very nearly equal in this study (to within 2 percent) by use of the ratio of pion to proton mass as found from a previous experiment.[5] An equality of velocities eliminates the necessity of knowing the exact value of q.

B. The Normalized Range

The factor that contributes most to the uncertainty in the determination of the mass of the pion is the statistical fluctuation in the ionization, which reflects in the total range of any particle. The particle ranges are distributed about a mean value in a manner that is essentially normal.[6] Therefore that function of the mass which is linear in the range is the quantity that is averaged; i.e.,

$$M^{1-q} = R_1 p^{-q}/c$$

where R_1 is the measured range. If one sets up the ratio of the average $\langle R_1 p^{-q} \rangle / c$ of the positive pion to that of the proton (for the same emulsion), the c cancels and

$$M_1{}^{1-q} = \langle R_1 p^{-q} \rangle / \langle R_1' p'^{-q} \rangle$$

where M_1 is the apparent ratio of the mass of the positive pion to that of the proton. The unprimed quantities represent those of the positive pion and the primed quantities are those of the proton. The expression Rp^{-q} is called the "normalized range." The ratio of the masses of the negative and positive pion is found in the same manner, i.e.,

$$\mathfrak{M}_1{}^{1-q} = \langle R_1 p^{-q} \rangle / \langle R_1' p^{-q} \rangle$$

where $\mathfrak{M}_1$ is the apparent ratio of the mass of the negative pion to that of the positive pion. Here the primed quantities are those of the positive pion and the unprimed those of the negative pion.

In order to determine whether the spread in the normalized range of the pions is consistent with their range straggling—to insure no other large sources of error—it is necessary to know their straggling in emulsion. It is convenient for this study that decaying pions provide a source of essentially* monoenergetic muons of ≃ 4.1 Mev (see Paper III). Of the positive pions that stopped in the film about 17 percent decayed into muons which lost all of their kinetic energy in the body of the emulsion. The ranges of these muons were measured and the straggling was calculated. This straggling was taken as a standard with which the straggling in the normalized range of the pions could be compared -- taking into consideration the difference in the masses of pion and muon. If the velocities of the pion and muon are equal then

$$\frac{\sigma_\pi^2}{\pi} = \frac{\sigma_\mu^2}{\mu}$$

where σ_π^2 and σ_μ^2 are, respectively, the variances in the distribution of ranges

*Occasional deviations from this monoenergeticity have been found by Fry and others.[7]

of pions of mass π and muons of mass μ. The above equality applies only to the so called Bohr straggling, to which most of the observed variance is attributed. Additional small contributions to the variance are discussed in Part V, A-5.

III. APPARATUS

A. The Magnetic Field of the 184-Inch Synchrocyclotron

The magnetic field intensity (H) of the 184-inch cyclotron has a gradual (and nearly linear) decrease from the center of the magnet to the 80-in. radius, beyond which point the decrease becomes very rapid (see Fig. 4). The standard value of the field at the magnet center is assumed to be 15,000 gausses and at the 80-in. radius is 94.6 percent of this. Therefore the orbits of particles produced from targets in the volume of the vacuum chamber of the cyclotron have varying radii of curvature. The centers of the orbits precess about the center of the cyclotron, resulting in trochoidal trajectories (see Paper I, Sec.III, A). These facts are of importance in calculating the momenta of particles.

B. The Circulating Proton Beam

The level of the circulating proton beam of the cyclotron varies as it expands radially. Both vertical and radial oscillations are present in the beam. The oscillations couple at the 81-in. radius and the beam loses stability. Thus targets are not placed beyond 81-in.

C. The Experimental Setup

1. Design of the particle "camera".

The velocity of the particles was the quantity that determined the dimensions of the particle camera. In order to compare range straggling it was necessary to have the velocities of the pions and protons approximately equal to that of the muons emitted in the decay of stopped pions ($\beta \simeq 0.27$).

The techinque of this study requires that the protons and pions be received in the film during the same exposure period. As in a previous experiment,[5] this was accomplished by mounting two targets on the apparatus. The targets were placed at such distances from the emulsion-coated plate that the $H\rho$'s of orbits terminating on the plate, from the nearer and more distant target respectively, would be in the ratio of the mass of the pion to the mass of the proton (see Fig. 1). The surface of the emulsion was placed slightly below the horizontal plane that passed through the centers of the targets. Thus detected particles entered the surface with well-defined entrance points. These particles, having left the target in a fairly flat downward-spiraling trajectory, entered the surface of the emulsion with a slight dip angle (which we called γ_1). The dip angle is defined as the angle between the emulsion surface and the path of the particles.

The apparatus was a refinement of previous designs. The entire assemblage was so constructed that a straight line from the center of the cyclotron passed through the centers of both targets and along the long axis of the plate. We called this the Central Radial Line. For purposes of reference and calculation a local rectangular coordinate system was adopted such that the x axis extended from the target along the Central Radial Line. The magnetic field was perpendicular to the xy plane.

2. The channels.

Limitations of space and considerations of background made it advisable to receive pions and protons on different parts of the plate. Consequently, after exposure to protons the proton target was removed and the entire assembly was moved 2 in. farther away from the center of the cyclotron so that the pions would be received at 80-in. (Fig. 2). Eighty inches from the center of the cyclotron was chosen as the distance for reception of the particles in order to have the highest bombardment energy on the targets and yet keep the orbits of the detected particles from going out to where the field falls off rapidly.

The apparatus was carefully designed to avoid contamination by pions not from the target and by those that scattered from the channel walls. The pion channels were built of copper around a central orbit 7-in. in diameter. The aperture of the channels permitted orbits of $\pm 10^{\circ}$ emission angle with respect to the local y axis through the target to enter. The channels were designed so that particles scattered from their walls could not enter the emulsion at the proper entrance angle ($\leqslant \pm 10^{\circ}$) for the desired particles. The proton channel was built around a central orbit 46.4-in. in diameter. The channel aperture allowed entry of orbits of $\pm 2^{\circ}$ emission angle with respect to the y axis through the proton target. The walls of these copper channels were lined with polyethylene, with the idea that the scattering of particles hitting the walls would be reduced. The channel assembly including the two targets and the nuclear track plate constituted the particle camera.

The camera was mounted on a large cart affixed to the end of the cyclotron probe (see Fig. 2). The probe was a cylindrical shaft of brass 12-ft. x 4-in. which passed into an air lock through a vacuum seal in the door. When the air-lock door had been clamped into place and vacuum had been established, the door to the vacuum chamber was opened and the probe was inserted into the cyclotron. The cart and apparatus were thus moved into position in the tank. Because the dimensions of the necessary proton orbit were greater than those of the air lock, the proton target was mounted on an extensible rod which was retracted while the equipment was in the air lock. When the cart was moved toward the center of the vacuum chamber, the rod was extended (by means of a length of strong vaccum-hose rubber under tension) until it was brought up against a positive stop when the target was the proper distance from the plate.

3. The targets.

The pion target consisted of a small rectangular parallelopiped of copper of width 2a = 0.044-in., length 2b = 0.832-in., and height 2c = 0.361-in. The width 2a was parallel to the Central Radial Line and the length 2b was parallel to the bombarding proton beam. The holder for the pion target was a thin 8-in. bar of brass with 1-1/4-in. arms projecting at each end. The target was suspended between the ends of these arms by means of 0.001-in. W. wire, which was under tension to keep the Cu target in place. No orbits from the body of the target holder could terminate on the plate; no particles from the bottom of the channel could enter the surface of the emulsion; any particle that scattered from the top of the channel and entered the emulsion would have too large a dip angle (γ_1) to be accepted.

The proton target was an 8-in. cylinder of 0.125-in. wolfram, fitted tightly into a vertical hole on the end of the extensible rod. It was firmly seated by means of a setscrew which clamped it into position. The effective height 2c of the target was obtained from the vertical spread of radioactivity over the cylinder after bombardment. The activity was found to be significant over a distance of 1-1/2-in. Thus 2c = 1.5-in.

The vertical spread in the bombarding beam must also be considered in pion production. There is a possibility of pion emission from the 0.001-in. W wires which suspend the pion target. Consideration of the volumes involved, however, lead one to expect only one pion from the wire for every 1,000 from the target.

4. The plate holder.

a. General. The experiment consisted of two parts. The plate holder was slightly different for the two. The plate holder was essentially a brass block 1-in.

x 3-in. x 3/8-in. Attached to the top edges were three small phospor-bronze leaf springs, which served to align the detector plate with respect to the top of the holder as well as to clamp it tightly in place and insure that it be flush with the top.

b. Part I. Since both positive and negative pions were to be detected, the top of the plate holder was in a horizontal plane. The height of the plate holder was governed by our decision to have the pitch angle (γ_o) of the spiral of the central orbits originating from the center of the target be $\approx 7^o$. The center of the pion target was 1.36-in. above the plane of the emulsion. We called this distance Z_o. The Z_o of the protons, however, was 0.61-in. (owing to the radial variation of the beam level). Thus γ_o for the protons was $\approx 0.5^o$.

c. Part II. In this part of the experiment only positive pions and protons were required. The pitch angle γ_o of the central orbits was reduced in order to reduce the error in the secant. This was accomplished by raising the channel assembly (with the plate holder) 0.38-in. Furthermore we wanted the pions to have about the same angle of dip as before in order to obtain a good estimate of it and yet insure that the pions stop in the film. Therefore a 2^o slant toward the positive channels was put in the top of the plate holder. The Z_o for pions was 0.98-in. and for protons 0.23-in. Here Z_o was the vertical distance from the center of the target to a horizontal plane through the long axis of the plate. We defined the angle of tilt as $\tan^{-1}\epsilon$.

d. The fiducial slits. The positions of the targets with respect to the entrance points of the particles were established by means of fiducial marks placed directly on the emulsion. This was accomplished with a slit system built into the apparatus as a part of the plate holder. The system consisted of two cross-shaped slits spaced 2-in. apart with the center of each 1/2-in. from the edges and adjacent end of the plate holder. The arms of the slits were aligned with the Central Radial Line to better than 0.2^o on a milling machine. Behind each of these slits was a small flashlight bulb. The bulbs were lighted for a few seconds after the detector plate was mounted (emulsion up) on the plate holder. A latent image of the slits was thereby left on the bottom surface of the emulsion. A phantom view of the plate holder, the fiducial slits, and the light-bulb container is shown in Fig. 3.

5. The Distance Measurements.

The distances from the targets to the respective fiducial slits were measured with respect to lines inscribed on a long brass bar. The bar was aligned parallel with the Central Radial Line and clamped tightly to the apparatus. Three lines were inscribed on the bar: one was near the pion fiducial slit, another near the pion target, and the last near the proton target. The distance from these objects to their adjacent scribe lines were measured by means of a micrometer microscope. The microscope was aligned so that its travel was parallel to the Central Radial Line. The distances between the lines on the brass bar were measured with an accuracy of ~ 1 part in 40,000 on a jig-boring machine. The distance between the pion and proton fiducial slits was measured separately with a traveling microscope. The pion fiducial slit was the principal reference slit. The proton fiducial slit was chiefly for the purpose of alignment. The uncertainty in the distances from the targets to the respective fiducial slits was $\approx$ 1 part in 10,000.

IV. PROCEDURE

A. The Exposures

The targets were bombarded for $\simeq$ 30 seconds each by the circulating proton beam. The bombarding energy on the proton target was $\approx$ 70 Mev.

The pion target was struck by $\approx$ 290-Mev protons. During the exposure to pions, the proton channel was plugged to eliminate background from scattered particles which might enter the channel. The protons received in the plate were those scattered in the backward direction (with respect to the beam direction) by the heavy W nuclei. The detected positive pions were emitted in the backward direction while the negatives were from the forward direction. The negative channel was plugged during the exposures for Part II of the experiment.

B. The Microscope Work

The exposed plates were developed and examined under high-power microscopes (98x and 12x) using oil-immersion objectives. The long axis of the plate was aligned with the lateral motion of the microscope stage by lining up the centers of the fiducial marks. (If the plate had been skewed during exposure, it was shimmed until the fiducial centers had a true lineup with the motion of the stage.) The coordinates, on the microscope stage, of the fiducial centers were recorded and the plates were scanned for the tracks of the desired particles. When these were found the coordinates of the first developed grain in the track were taken. The angle of the track with respect to a local y axis through that point was measured with an eyepiece goniometer. The range of the particle was measured by recording the length of successive straight segments of track as measured either on a calibrated eyepiece reticle or on the verniers of the stage.* The depth of penetration into the emulsion between the beginning and end of each segment of track was measured by means of the micrometer fine adjustment. A correction was applied to the depth measurement since emulsion shrinks on being processed. A study of emulsion shrinkage under fairly wide ranges of humidity and temperature has been made.[8] A shrinkage factor of 2.3 ± 0.1 seems best for the conditions of humidity and temperature at Berkeley and was used throughout the experiment.

C. The Momentum Calculation

1. Measurement of H.

The magnetic field (H) of the cyclotron was measured by means of a nuclear fluxmeter, which measures the precession frequency of protons in a hydrogenous material placed in the magnetic field.[9] The measurement was taken the same day as the particle exposures were made and while the exiting current of the magnet was maintained constant. It was performed in vacuo and was made along the cyclotron-probe center line. Many determinations were made and it was found that the relative variation of the field with cyclotron radius remained constant, although the absolute values varied slightly from day to day. This study did not require knowledge of the absolute values of the field since, essentially, only the <u>ratio</u> of momenta was involved. In order to find the decay momentum of the muon, however, the absolute values were required (see Paper III). An azimuthal measurement was taken along the proton orbit. It was found that the radial variation of the field along the proton orbit was the same as that along the probe line. The

---

* Three observers took data in this experiment. One measured tracks by means of the eyepiece reticle, the other two used the verniers of the microscope. (Displacements of the stage could be read directly in microns.) Great care was taken to insure that all three were using comparable standards. Many cross checks were made: One observer measured a track using his microscope and method and then the plate was given to another observer who used his technique to measure the same track. In all cases the difference found was of the same order as the error in measurement for a single observer ($\simeq 0.1 \times R^{1/2}$). Since any one observer measured pion and proton ranges by the same method, an absolute calibration of his range scale was not necessary for finding the <u>ratio</u> of the masses. The subsidiary study of the muon range straggle, however, required the absolute measurement (also see Paper III).

variation was slightly different on the other side of the probe line along the mirror image of the proton orbit. This difference may have been caused by a perturbation in the field due to the proximity of the vacuum-tank wall. This difference, however, was not observable over the orbits of the pions. The results of these measurements are shown in Fig. 4. The relative values of the field over the orbits were measured to an accuracy of 0.01%. Figure 4b shows the percent difference between the field along the proton orbit and the field along the mirror image of the orbit in percent gauss. The error envelope is included.

2. The calculation of $H\rho$.

The calculation of $H\rho$ involves integration of the expression

$$K = \frac{\int_{r_1}^{r_1 + x_o} rHdr}{r_1 \cos(\theta' + \lambda_o) + (r_1 + x_o)\cos\theta'}$$

from the target to the plate (see Paper I, Sec. III). In this expression r_1 is the distance from the center of the cyclotron to the target and x_o is the distance from the target to the point of reception of the particle on the x axis (see Fig. 5). The angle $(\theta' + \lambda_o)$ is the emission angle with respect to the local y axis at the target and θ' is the reception angle with respect to the y axis at the point at which the particle orbit crosses the x axis. The angle of precession of the center of the orbit about the center of the cyclotron is the angle λ_o.*

The results of this type of calculation can be expressed in graphical form; the labor involved in the calculations therefore was reduced.

The apparent $H\rho$ was calculated on the assumption that the particles came from the center of the target. In calculating the effect of the finite target size, the assumption was made that the particles came with equal probability from each element of the target volume. This assumption was justified by the results of bombarding a test target and checking the radioactivity throughout its volume. A test target was used that was of the same dimensions as the actual pion target, but it consisted of four 0.011-in. layers stamped together. After bombardment

*Because the field is nearly uniform the expression for K is insensitive to r_1 and therefore to the exact location of the target-detector assembly in the magnetic field. If the field is uniform $\lambda_o = 0$ and the integration gives $K = Hx_o/2 \cos\theta'$, which is independent of r_1.

by the circulating proton beam the four layers of the test target were separated and the activity was checked. The activity was the same on the four sections, which indicated that the centroid of activity was the center of the target. The graphical representation used in the calculation (the numerical integration of

$$(H\rho)_o = (K)_o \sec \gamma_o = \frac{\sec \gamma_o}{2r_1 + x_o} \int_{r_1}^{r_1 + x_o} rHdr \;)$$

was for orbits received at $\theta' = 0^o$. γ_o is that nominal value of the pitch angle of the helical orbits defined by $\tan \gamma_o = 2 Z_o/\pi x_o$. The distribution of the true value of the pitch angle (γ) around γ_o was included in the calculation of the effect of the finite target and detector dimensions. (See Sec. IV)

If the particle found entered the plate on either side of the radial line at an angle θ with respect to a local y axis through that point, then $r_1 + x_o = 80 + \Delta x + y' \tan (\theta - \alpha')$ (see Fig. 5). The small part of the orbit from the point where the particle entered the plate to the point at which it crossed the Central Radial Line was in an essentially uniform field-- the maximum variation was 0.07 percent. Therefore the projection of the orbit (the small distance $y' \tan \{\theta - \alpha'\}$) on the radial line was calculated for a circle. The $H\rho$ found from the graph was then corrected for the angle θ' that the particle made with the y axis as it crossed the Radial Line and for the emission angle $(\theta' + \lambda_o)$. For the small orbits of the pions $\lambda_o \simeq -0.2^o$, thus $\theta' + \lambda_o \simeq \theta'$. The larger orbit of the protons precessed $\simeq -1.5^o$. Therefore $\theta' + \lambda_o = \theta' - 1.5$. The actual magnetic rigidity was then $(H\rho)_{\theta'} = (H\rho)_o \sec \theta'$ for pions

$$\text{and} \quad (H\rho)_{\theta'} = (H\rho)_o \left(\frac{1.9997\, r_1 + x_o}{r_1 \cos (\theta' - 1.5) + (r_1 + x_o) \cos \theta'} \right)$$

for protons. These expressions are good approximations to $H\rho = K \sec \gamma_o$ where K is the exact expression given at the beginning of this section.

V. ANALYSIS OF THE DATA

A. Range Straggling of Muons in Nuclear Track Emulsion

1. General.

The particles used for this subsidiary study were the positive muons arising from decay of stopped positive pions. The method of measurement was the same as for the other tracks. The measurement began from the terminus of the positive pion track. Those muon tracks which showed large scatters were eliminated from the study because they might have suffered appreciable energy loss during the scatter.

During the course of the study, tracks of 558 positive muons that had expended their kinetic energy in the body of the film were examined.

2. Expected difference between the observed distribution and that in an infinitely thick film.

The probability that a given track will stop in the emulsion depends on its length. The staying-in probability is $\approx t/2R$ where $t(< R)$ is the thickness of the film and R is the range of the particle. Consider an observed distribution of muon ranges in a film of thickness t. Let n_i be the observed number of tracks with range R_i and $\langle R_\mu \rangle$ the mean of the observed distribution. One can arbitrarily let the observed number of tracks of range $\langle R_\mu \rangle$ be the number that would be found in an infinite emulsion. The number of tracks with range R_i that would be observed in the infinite emulsion is

$$(n_i)_o = \left(n_i \frac{R_i}{\langle R_\mu \rangle} \right)$$

where the correction factor is simply the ratio of the staying-in probability of the track of range R_i to that of the tracks of range $\langle R_\mu \rangle$. The corrected distribution will then have a mean

$$\langle R \rangle_o = \frac{\sum_i (n_i)_o R_i}{N} = \frac{\sum_i n_i \left(\frac{R_i}{\langle R_\mu \rangle} \right) R_i}{N}$$

where N is the total number of tracks in the distribution. If one adds $2 \langle R_\mu \rangle$ and subtracts $2\sum_i n_i R_i/N$ (which is $2\langle R_\mu \rangle$), one has

$$\langle R_\mu \rangle_o \doteq \langle R_\mu \rangle + \frac{\sigma_\mu^2}{\langle R_\mu \rangle} \quad \text{Where } \sigma_\mu^2 = \sum_i \frac{n_i (R_i - \langle R_\mu \rangle)^2}{N}$$

(the observed variance). In this study $\frac{\sigma_\mu}{\langle R_\mu \rangle} \simeq 4.5$ percent and $\langle R_\mu \rangle \simeq 600\mu$. Thus the mean of the distribution is increased $\simeq$ one micron by the staying-in correction.

3. Normalization of the emulsions.

The events examined in this study were sampled from 12 plates. Since the stopping power varied from plate to plate, it was necessary to normalize the emulsions. The ranges of the muons in the individual plates were normalized to the same mean. In the previous section it was shown that the correction for the staying-in probability raises the mean $\simeq$ 1 micron. For this reason a mean of 599 microns was used a posteriori to normalize the tracks (in order to obtain 600 microns as the arbitrarily chosen mean of the final distribution). The observed ranges were normalized to a mean of 599 microns by means of the formula:

$$R_{iN} = R_{ij} \left(\frac{599}{\langle R_j \rangle} \right)$$

where R_{ij} and $\langle R_j \rangle$ were respectively the observed i-th range and the mean for the j-th plate. Then R_{iN} is the normalized i-th range.

4. Correction for the thickness of film.

The correction to the normalized distribution for the probability of the particles' stopping in the film was

$$(n_i)_o = n_i \left(\frac{R_i}{600} \right)$$

where n_i was the number of events in the i-th range interval in the histogram of the distribution and R_i was the central range for that interval. Then $(n_i)_o$ is the corrected frequency for that interval.

5. The Straggling.

Figure 6 shows the final distribution of the ranges of the 558 tracks measured for this study. The mean of the final distribution was 600 microns. The amount of straggling, shown in Fig. 6, was 4.5_3 percent. In Appendix I it is shown that this is higher than the true straggle by only $\simeq 0.01$ percent. The total straggling to be expected from the Bohr straggling for the emulsion used, the straggling due to the heterogeneous character of the emulsion, and the straggling due to observer error (see Paper I, eq. 25) was 4.0 percent. The difference between this value and that actually observed may be due to the distortion produced in the emulsion by the loss of a fairly large volume of silver upon processing. One can expect two types of distortion: the large-scale distortion produced by strains developing in the emulsion during the fixing and drying processes, and the small-scale distortion resulting from the nonuniform removal of silver halide. The latter distortion arises from the collapse of small cells when the silver is removed and a stretching of their neighbors. The shrinkage or stretching is random in nature. This small-scale distortion produces a variance in the range of particles which one would expect to be proportional to the range. The large-scale distortion can be relieved considerably by good processing technique but the small-scale distortion is an inevitable result of the nonuniform removal of silver. It would be expected that a thicker emulsion would have a greater large-scale distortion and the variances of the muon range distribution would be larger. This seems to be the case.*

An additional amount of straggling might be expected from the pion's decaying while still in motion after producing the last grain ($\beta \simeq 0.017$). A calculation of the upper limit to the time it takes the pion to slow to thermal velocities (assuming it loses its energy only by elastic collisions with protons) is $\approx 2 \times 10^{-12}$ seconds. Since the mean life of the pion is 2.5×10^{-8} sec.,[10] the probability of a decay's occuring in the estimated time interval is exceedingly small. Thus the contribution to the range straggling from decay in motion is negligible.

6. The asymmetry in the distribution of ranges.

The amount of skew in the range distribution to be expected from Lewis's prediction[6] is small ($\simeq -0.03$). An additional amount of skew due to a possibility of inner bremsstrahlung during the pi-mu decay process[7] might be expected. An

---

* A. M. Siefert, Private Communication to W. H. Barkas

estimate* of this skew yields $\simeq$ -0.001. The skew from these effects, then, is not inconsistent with that found for the observed distribution (-0.03 ± 0.12), although such a small skew is masked by the statistical error. (The skews quoted are dimensionless quantities, i.e., the ratio of the third moment about the mean to the cube of the standard deviation.)

B. Straggling in the Normalized Range of Pions

In order to insure that only pions were measured, the tracks chosen for measurement were those negative tracks which terminated in stars (negative muons rarely produce stars[12]) and those positive tracks which showed a definite decay secondary. (Since C-2 emulsion is not sensitive enough to render electron tracks developable, the electron emitted in the decay of a stopped muon is not seen.)

The quantity studied statistically was $cM^{1-q} = R_1 p^{-q}$ (the normalized range). The R_1 in the expression is the measured range corrected for the probability that the first developed grain in the track did not lie on the surface of the emulsion (see Paper I, Sec. IV, C-4). The correction is equal to the average grain spacing at the beginning of the track. This grain spacing was 0.9 microns. This might seem somewhat surprising for C-2 emulsion (particle $\beta \simeq 0.26$), but the surface layer was presensitized by a small amount of light leakage due to a glow in the tank at the time of exposure. The amount of correction to the range of pions ($\langle R \rangle \simeq 725\mu$) was 0.124 percent and for protons ($\langle R \rangle \simeq 4580\mu$) was 0.020 percent.

The p in the normalized range is the magnetic rigidity and not the momentum. The factor by which they differ (e/c) is absorbed in the constant c which multiplies M^{1-q}.

When the magnetic rigidity had been determined (see Sec. IV, C) and the range had been measured for each particle, the normalized range was calculated and the mean was evaluated for each plate studied.

Figures 7 and 8 show the distributions of the normalized ranges of pions from parts I and II respectively of the experiment. All tracks meeting the angle criteria are shown.

*The probability function given by Eguchi[11] was approximated for range losses up to 90 microns (the interval in which ranges were observed). The approximation was then used to calculate the additional skew and additional variance produced in the range distribution. The additional straggling due to inner bremsstrahlung as found from this calculation was $\simeq$ 0.008 percent.

Table I lists the means of the normalized ranges and the actual straggling calculated for each of the six plates studied. The existence of a variation in the stopping power from plate to plate is seen in the normalized ranges of the pions and protons. The ratio of the normalized ranges, however, is nearly constant (see Table II).

The theoretical straggle in the normalized range was calculated using Bohr straggle, heterogeneity straggle, observer error, target size corrections, (see Paper I, Eq. 28) and the straggle expected from distortion effects.

The amount of distortion straggling was calculated assuming $\sigma_d^2 = kR$ (see Paper I, Sec. IV). The k was assumed to be constant and dependent only upon the emulsion used. The value of k was found from the difference between the observed straggle of the muon range distribution (see the previous section) and the straggle predicted by the first three terms of the theoretical straggle mentioned in the previous paragraph. The predicted straggle for the normalized ranges of pions was 4.0 percent. The observed mean straggle for the six plates studied (Table I) was (4.1 ± 0.1) percent.

The same type of analysis of the normalized range was carried out for the protons received in the plates. An expected straggle of 1.3 percent was calculated,* whereas the mean observed straggle determined in the six plates was (1.2 ± 0.1) percent. These values are certainly statistically compatible. The sample, however, was rather small--it consisted of 60 protons, 10 on each of the plates.

Figure 9 shows the distribution of the normalized ranges of the protons. The distribution was normalized to a mean of 68.0×10^{-22} for comparison.

The agreement between the predicted straggling in the normalized ranges of pions and protons and the straggling actually observed leads one to believe that no tracks that could be considered extraneous were found.

C. The Masses of the Charged Pions

1. The positive pion.

The quantity $M_1 = \left(\dfrac{\langle R_1 p^{-3.44}\rangle}{\langle R_1' p'^{-3.44}\rangle}\right)^{-1/2.44}$ was calculated for each of

*For an infinite emulsion one would calculate 1.5 percent as the expected straggle in the proton ranges. However, since the emulsion used was only 200 microns thick and the proton ranges were ≈ 4600 microns, most of the track lay in the region where the emulsion-glass adhesion would limit the small-scale distortion. Therefore the effect of this distortion has been neglected in the calculation.

the six plates containing positive pions and protons. The unprimed quanitites refer to pions and the primed to protons. M_1 is the apparent ratio of the mass of the positive pion to the mass of the proton. Or it is the uncorrected mass of the positive pion in units of the proton mass. This mass differs from the "actual" mass M by a factor:

$$M = M_1 \left(1 + \frac{e_1 - e_1'}{q - 1} + \frac{w_q - w_q'}{q - 1} \right) .$$

The e_1 is the Lewis Effect (see Paper I, Sec. IV, C-1) on the mean ranges, w_q is the effect of the finite target size on the momenta.

The mean ratio of the mass of the positive pion to that of the proton and its variance calculated for each plate are shown in Table II.

The e_1 increased the ranges of pions ($\beta \simeq 0.26$) by 0.197 percent and e_1' increased the proton ranges by 0.029 percent. Thus the increase in the apparent positive pion mass due to this effect was $e_1 - e_1' / q - 1 \doteq 0.168\% / 2.44 = 0.069\%$.

Since the targets were uniformly illuminated with beam protons (see Sec. III), the only terms of significance in the corrections to the momenta (see Paper I, Sec. III, B) were given in Table I of Paper I. Substituting these quantities into the expression given by Barkas for w_q, one has:

$$w_q = \frac{q}{x_o^2} \left[\frac{q-1}{2} \cdot \frac{a^2}{3} + \frac{b^2}{3} + \frac{6}{\pi^2} \cdot \frac{c^2}{3} + \frac{8}{\pi^3} \left(Z_o^2 + c^2 \right) \left(\langle \theta' \rangle + \frac{\langle y' \rangle}{x_o} \right) + \right.$$

$$\left. \frac{4 x_o \epsilon}{\pi^2} \left(\frac{c^2}{3 Z_o} + Z_o \right) \frac{\langle y' \rangle}{x_o} \right]$$

As defined in Sec. III:

2a = the width of the target

2b = the length of the target

2c = the height of the target

Z_o = the vertical distance from the center of the target to the horizontal plane along the surface of the emulsion.

ϵ = the tangent of the angle of tilt of the emulsion surface.

for the cylindrical proton target of radius r_o we substitute,

$$\frac{a^2}{3} = \frac{b^2}{3} = \frac{r_o^2}{4} .$$

The first three terms are constant and depend only on the dimensions involved in the apparatus. Although Z_o and ϵ were not the same for parts I and II of the experiment (see Sec. III, C-4), $\langle\theta'\rangle$ and $\left\langle\frac{y'}{x_o}\right\rangle$ were the only statistical variables on the six plates. The correction to the mass of the positive pion for this effect was then

$$\frac{w_q - w'_q}{2.44} \approx 0.025\%. \qquad \text{(see Appendix II)}$$

The total amount of correction to the positive pion mass, which involved these effects as well as the correction to the range for the grain spacing, came to ≈ 1 part in 2,000.

The variances in the masses were calculated by means of Eq. 31, Paper I, i.e.,

$$\sigma_M^2 = \left(\frac{M}{q-1}\right)^2 \left[\frac{\sigma^2}{n\left\langle R_1 p^{-q}\right\rangle^2} + \frac{\sigma'^2}{n'\left\langle R'_1 p'^{-q}\right\rangle^2} + \frac{\sigma_q^2}{4}\left(\frac{\sigma_p^2}{\langle p\rangle^2} - \frac{\sigma_{p'}^2}{\langle p'\rangle^2} - 2r\right)^2 + \frac{\sigma_S^2}{S^2}\left(\left\langle \sin^2\gamma_1\right\rangle - \left\langle \sin^2\gamma'_1\right\rangle\right)^2\right]$$

The σ^2 is the variance in the normalized range of the particles (unprimed quantities refer to pions, primed to protons).

σ_q is the uncertainity in q (3.44 ± 0.03).

σ_p^2 is the second moment in the distribution of momenta of mean $\langle p\rangle$.

r is defined as: $M(1 + r) = \langle p\rangle / \langle p'\rangle$.

σ_S is the uncertainty in S (2.3 ± 0.1).

γ_1 is the angle of dip into the emulsion of the track.

The first two terms (including the factor $\left\{\frac{M}{q-1}\right\}^2$) are simply the variance in the mass due to the straggle in the normalized ranges of pion and proton. The third term is the uncertainty in the mass due to the uncertainty in q over the spread of momenta observed. In all six plates $\frac{\sigma_p^2}{\langle p \rangle^2} - \frac{\sigma_{p'}^2}{\langle p' \rangle^2}$ was negligible compared to $r = \left(\frac{\langle p \rangle / \langle p' \rangle}{M} - 1\right)$, which was ≈ 0.02. The last term is the uncertainty in the mass due to the uncertainty in the shrinkage factor (S)--which reflects in vertical components of the ranges. A measurement of the angle of descent into the emulsion of small, straight segments of tracks of 40 pions yielded $\langle \sin^2 \gamma_1 \rangle = 0.015$, and for protons $\langle \sin^2 \gamma_1' \rangle$ was 0.001. The first two terms are of the order of 1.5×10^{-7}, the third $\approx 0.016 \times 10^{-7}$ and the last $\approx 0.003 \times 10^{-7}$. Thus the dominant term in the spread of the mass is the range straggling.

The final weighted mean and its variance are shown at the bottom of Table II. The weighted mean was found by the well-known expression $\mu = \sum_i w_i \mu_i$ where μ = weighted mean of i determinations of the mean μ_i with variance σ_i^2 and weight w_i, $\sigma^2 = \sum_i w_i^2 \sigma_i^2$ (follows from the definition of variance).

Here $w_i = \frac{1/\sigma_i^2}{\sum_i \left(1/\sigma_i^2\right)}$ (found by minimizing the variance with respect to the weight w_i and using a Lagrangian multiplier on the constraining conditions, $\sum_i w_i = 1$). Assuming a value of 1836.1 m_e for the mass of the proton,[13] the derived mass of the positive pion in electron masses is: 273.3 ± 0.2 where the error has been converted into a probable error.

2. The negative pion.

The quantity $\mathcal{M}_1 = \left(\frac{\langle R_{1p}^{-3.44} \rangle}{\langle R_{1}' {p'}^{-3.44} \rangle}\right)^{-1/2.44}$ was calculated for each of the three plates that contained both negative and positive pions. Here the unprimed quantities are those of the negative pion while the primed quantities refer to those of the positive pion. Then $\mathcal{M}_1$ is the apparent ratio of the mass of the negative pion to that of the positive pion. The difference between this ratio and the "actual" ratio is negligible, since the three effects discussed in the previous section essentially cancel.

The mean ratio of the masses and its variance calculated for each plate are given in Table III.

Again the variances were calculated using Eq. 31, Paper I (see the previous section). Here the first two terms are the variance in the ratio of masses due to the normalized range straggling of the two pions. The third term is negligibly small and the last term is zero.

The final weighted mean of the ratio of the mass of the negative pion to that of the positive pion and its variance are shown at the bottom of Table III. The weighted mean was found as in the previous section. This ratio is 0.997 ± 0.002. Prof. E. Fermi* has made a calculation for pions in the C-2 emulsion based on the Mott theory of scattering,[14] which predicts a difference in stopping cross section for particles of opposite sign. Fermi shows that the negative-to-positive pion-mass ratio will apparently be reduced by ≃ 0.1 percent. A correction for this expected difference in stopping cross section was applied to our data and the final ratio is shown at the bottom of Table II--a value of 0.998 ± 0.002.

VI. DISCUSSION OF RESULTS

In an earlier report[15] the mass of the negative pion was given in units of the proton mass. Upon a review of the data** it was decided to consider the experiment from a slightly different point of view.

It is believed that the ratio of the mass of the positive pion to that of the proton as shown in Table I is a reliable value for that quantity. There were two independent experiments (performed on different days) involving three separate exposures each. Thus there were actually six different experiments on the measurement of the mass of the positive pion. The apparatus had to be newly positioned before each exposure, therefore the exposures were not identical in absolute position and magnetic field intensity. The target used in part I was not the same (although the dimensions were approximately the same) as that used in part II. The mean ratio of the positive pion mass to the proton mass in part I was 0.14895 ± 0.00024. The ratio in part II was 0.14873 ± 0.00022. These results are well within statistics and show that the two determinations are equivalent. The ratios in the individual plates are all quite consistent and the ratio of external error to internal error[16] for the six plates is 1.0 ± 0.2. In addition, the sign of the positive pion charge is the same as that of the proton, so that a possible dependence of the stopping cross section upon the sign of the charge does not complicate the matter.[14] Thus it was decided to regard the ratio of the mass of the positive pion to that of the proton as the fundamental measurement of the mass of the pion.

---

*E. Fermi, private communication to W. H. Barkas.

**The maximum value of θ' accepted was slightly reduced in order to reduce the error in the momenta.

Next an investigation was made into the apparent ratio of the masses of the negative and positive pions, making use of the data obtained from the three plates that were exposed simultaneously to positive and negative pions. A number of possible sources of systematic error thus were eliminated, since the particles had come from the same target during the same bombardment interval and the apparatus was completely symmetrical for the reception of the two types of particles. For this reason geometrical factors were excluded and the ratio of the masses was obtained essentially from the observed ratio of the normalized ranges. The statistical error is slightly higher than that of the previous calculation since the range straggling of the comparison particle is larger.

In Table III, it is to be noted that two of the plates give a ratio of negative to positive pion mass that is very nearly equal to 1.000. The third (plate No. 27152) indicates a ratio of masses of 0.9908 ± 0.0032, an amount that might be considered significantly different from the other two. Examination of the data revealed nothing to throw doubt upon the result, therefore it has been included. Although the ratio of external error to internal error for the three plates is 1.6 ± 0.3, the internal error was used, as no reason could be found for suspecting a large systematic error.

A small effect that might cause an apparent increase of the negative-pion normalized range would be contamination by negative muons from decay of the pion in flight. The probability for this is very small because of the stringent criteria used ($\pm 10^{\circ}$ entrance angle, $\simeq 7^{\circ}$ dip angle, and star formation). At the most an increase of $\simeq$ 1 micron in the mean range could be expected.

TABLE I

SUMMARY OF THE NORMALIZED RANGE DATA

		POSITIVE PIONS			PROTONS			NEGATIVE PIONS		
	Plate Number	Number of Events	Mean Normalized Range (x 10^{20})	Standard Deviation (percent)	Number of Events	Mean Normalized Range (x 10^{22})	Standard Deviation (percent)	Number of Events	Mean Normalized Range (x 10^{20})	Standard Deviation (percent)
Part I:	27152	56	70.13	(4.5±0.4)%	10	67.18	(1.2 ±0.2)%	54	71.73	(3.7±0.4)%
	27153	49	70.85	(3.7±0.4)%	10	67.29	(1.2 ±0.2)%	49	70.97	(4.7±0.5)%
	27154	51	70.77	(4.2±0.4)%	10	68.31	(1.2 ±0.2)%	44	70.57	(4.0±0.4)%
Part II:	28848	65	70.85	(3.8±0.3)%	10	68.07	(1.1 ±0.2)%			
	28849	69	72.47	(3.7±0.3)%	10	68.72	(1.5 ±0.3)%			
	28853	78	70.74	(4.6±0.4)%	10	67.41	(1.0 ±0.2)%			
	Totals	368			60			147		

Mean Normalized Range = $\left\langle R_1 p^{-3.44} \right\rangle$, R in microns, p in gauss m.m.

Mean Straggle of the Normalized ranges of pions = (4.1 ± 0.1)% (515 events)

Mean Straggle of the Normalized ranges of protons = (1.2 ± 0.1)% (60 events)

TABLE II

SUMMARY OF THE RESULTS ON THE RATIO OF THE MASS OF THE POSITIVE PION TO THAT OF THE PROTON,

	Plate Number	Number of Events	Ratio of the Masses (M)	Variance of the Ratio (σ_M^2)	Standard Deviation (σ_M)
Part I:	27152	56	0.14902	19.20×10^{-8}	±0.00044
	27153	49	0.14847	15.94×10^{-8}	±0.00040
	27154	51	0.14944	18.85×10^{-8}	±0.00043
Part II:	28848	65	0.14914	12.98×10^{-8}	±0.00035
	28849	69	0.14833	15.87×10^{-8}	±0.00040
	28853	78	0.14864	14.02×10^{-8}	±0.00037

(10 protons on each plate)

$$\langle \sigma_M^2 \rangle = 2.64 \times 10^{-8}$$

$$\langle M \rangle = 0.14883 \pm 0.00016$$

The errors shown are standard deviations.

Using 1836.1 m_e as the Mass of the proton, then:

$$\boxed{m_{\pi^+} = (273.3 \pm 0.2)\, m_e}$$

where the final error shown has been converted to a probable error.

TABLE III

SUMMARY OF THE RESULTS ON THE RATIO OF THE MASS OF THE NEGATIVE PION TO THAT OF THE POSITIVE PION,

	Plate Number	Number of Events		Ratio of the Masses ($\mathcal{M}$)	Variance of the Ratio ($\sigma_{\mathcal{M}}^2$)	Standard Deviation ($\sigma_{\mathcal{M}}$)
		π^-	π^+			
	27152	54	56	0.9908	10.15×10^{-6}	±0.0032
Part I:	27153	49	49	0.9993	12.26×10^{-6}	±0.0034
	27154	44	51	1.0009	11.94×10^{-6}	±0.0034

$$\langle \sigma_{\mathcal{M}}^2 \rangle = 3.79 \times 10^{-6}$$

$$\langle \mathcal{M} \rangle = 0.9966 \pm 0.0020$$

On making the Fermi correction for the difference in stopping-cross section we obtain:

$$\boxed{\pi^-/\pi^+ = 0.998 \pm 0.002}$$

The errors shown are standard deviations.

APPENDIX I

The effect upon the value of the range straggling of muons due to normalizing all plates to a mean of 599 microns.

It is reasonable to assume that if a number of batches of emulsion were sampled, it would be found that the effective number of particle-stopping electrons per unit volume would be distributed in a narrow Gaussian distribution. The mean of this distribution can then be chosen as the number of stopping electrons per unit volume in a "typical" emulsion. Let $\langle R_o \rangle$ be the true mean of the muon-range distribution in this emulsion.

Suppose there are n samples of emulsion, each with a muon-range distribution. In order to normalize each plate to the typical emulsion, a normalizing factor k_j must be found for each of the n plates. The k_j will be the ratio between the number of stopping electrons in the j-th plate and that in the typical emulsion. Then $k_j R_{ij} = R_i$ where R_{ij} is the i-th range in the j-th plate, k_j is the normalizing factor for the j-th plate and R_i is the range the i-th particle would have had in the typical emulsion.

Now $k_j = \langle R_o \rangle / \langle R_j \rangle$ where $\langle R_j \rangle$ is the true mean of the distribution in the j-th plate. Then the true variance of the distribution of all events is

$$\sigma^2 = \frac{\sum_{j=i}^{n} \sum_{i=1}^{n_j} \left(k_j R_{ij} - \langle R_o \rangle\right)^2}{\left(\sum_{j=1}^{n} n_j\right)}$$ where n_j = no. of events on the j-th plate or

$$\sigma^2 = \frac{\sum_{j=1}^{n} \sum_{i=1}^{n_j} \left(\langle R_o \rangle / \langle R_j \rangle\right)^2 \left(R_{ij} - \langle R_j \rangle\right)^2}{N}$$ where $N = \sum_{j=1}^{n} n_j$ = total no. of

particles in the study and the true relative variance (σ_R^2):

$$\sigma_R^2 = \frac{\sigma^2}{\langle R_o \rangle^2} = \frac{\sum_{j=1}^{n} \sum_{i=1}^{n_j} \frac{\left(R_{ij} - \langle R_j \rangle\right)^2}{\langle R_j \rangle^2}}{N} \equiv \frac{\sum_{j=1}^{n} \sum_{i=1}^{n_j} \frac{\left(\Delta r_{ij}\right)^2}{\langle R_j \rangle^2}}{N}$$

Now $\langle R_j \rangle$ is not known, as there was but a single estimate of it from the range distribution on the j-th plate. Let $\langle R_j \rangle_e$ be this estimate. Then:

$$\langle R_j \rangle_e = \langle R_j \rangle + \epsilon_j \ .$$

Placing $\langle R_j \rangle_e$ in the expression for the relative variance instead of $\langle R_j \rangle$; one finds that the relative variance is slightly higher than the <u>true</u> relative variance:

$$\sigma^2_{R(\text{apparent})} = \sigma^2_{R(\text{true})} + \frac{\sum_{j=1}^{n} \sum_{i=1}^{n_j} \left(\frac{\epsilon_j}{\langle R_j \rangle} \right)^2 \left(\frac{3\,(\Delta r_{ij})^2}{\langle R_j \rangle^2} + 1 \right)}{N}$$

where, in the case of normalizing to 599 microns,

$$\frac{\sum_{j=1}^{n} \sum_{i=1}^{n_j} \left(\frac{\epsilon_j}{\langle R_j \rangle} \right)^2 \left(\frac{3(\Delta r_{ij})^2}{\langle R_j \rangle^2} + 1 \right)}{N} \simeq 0.03 \times 10^{-4}$$

Thus normalizing the emulsions has essentially no effect upon the relative variance.

APPENDIX II

Calculation of the correction to p^{-q} due to the finite size of the target and detector.

In Section III the dimensions of the targets were given:

(dimensions in inches)

Pion target (parallelopiped)	Proton target (cylindrical)
$a = 0.022$	$a = b = \sqrt{3/4}\ r_o = 0.0555$
$(x_o = 7.00)$ $b = 0.119$	$(x_o = 46.4)$ $c = 0.75$
$c = 0.1805$	

	Pion target	Proton target
Part I	$Z_o = 1.36$	$Z_o = 0.61$
	$\epsilon = 0.00$	$\epsilon = 0.00$
Part II	$Z_o = 0.98$	$Z_o = 0.23$
	$\epsilon = 0.035$	$\epsilon = 0.035$

Placing these values in the expression given in Section V, C-1, one has:

Part I

$$w_q = 7.02 \times 10^{-2} \left[1.15 \times 10^{-2} + 0.49 \left(\langle\theta'\rangle + \frac{\langle y'\rangle}{x_o}\right)\right]$$

$$w_{q'} = 1.60 \times 10^{-3} \left[0.116 + 0.24 \left(\langle\theta'\rangle + \frac{\langle y'\rangle}{x_o}\right)\right]$$

Part II

$$w_q = 7.02 \times 10^{-2} \left[1.15 \times 10^{-2} + 0.26 \langle\theta'\rangle + 0.10 \frac{\langle y'\rangle}{x_o}\right]$$

$$w_{q'} = 1.60 \times 10^{-3} \left[0.116 + 0.16 \langle\theta'\rangle + 0.69 \frac{\langle y'\rangle}{x_o}\right]$$

From the six plates studied it was found that:

For Pions		For Protons	
$\langle \theta' \rangle$	$\frac{\langle y' \rangle}{x_o}$	$\langle \theta' \rangle$	$\frac{\langle y' \rangle}{x_o}$
-9×10^{-3}	-2×10^{-3}	4×10^{-3}	2×10^{-3}
-3×10^{-2}	3×10^{-3}	3×10^{-2}	3×10^{-3}
2×10^{-3}	-3×10^{-3}	4×10^{-2}	2×10^{-3}
1×10^{-2}	-1×10^{-2}	2×10^{-2}	2×10^{-3}
3×10^{-3}	1×10^{-2}	6×10^{-3}	4×10^{-3}
1×10^{-2}	-6×10^{-4}	1×10^{-2}	2×10^{-3}

Thus the finite target size increased the p^{-q} of the pions by ≈ 0.081 percent over the p^{-q} calculated from the center of the target. The increase in p'^{-q} for protons was ≈ 0.019 percent.

ACKNOWLEDGMENTS

I wish to express my gratitude to the many persons who assisted in the completion of this work. Mrs. T. W. Griswold did a substantial amount of the scanning and much of the calculating. Dr. W. H. Barkas and Dr. W. Birnbaum were active in all phases of the experiment. Mr. W. W. Connover built and aligned most of the apparatus. Mr. J. McFaden built the extensible proton target holder. I am grateful to Dr. Barkas and Dr. Birnbaum for many helpful suggestions and edifying discussions. The computing group at the laboratory gave great aid in completing the calculations. Mr. J. T. Vale and the cyclotron crew made the bombardments. Throughout the study Professor E. O. Lawrence has given his support.

The memory of Dr. E. Gardner, one of those who pioneered the program, has been with us during this last part of the study.

REFERENCES

1. The Cosmic Ray Conference at Bagnères de Bigorre, July 6-12, 1953.
2. E. Gardner and C. M. G. Lattes, Science 107, 270 (1948).
3. E. Gardner and C. M. G. Lattes, Phys. Rev. 74, 1236 A (1948).

   W. H. Barkas, E. Gardner, and C. M. G. Lattes, Phys. Rev. 74, 1558 A (1948).

   A. S. Bishop, E. Gardner, and C. M. G. Lattes, Phys. Rev. 75, 1468 A (1949) (3 Papers).

   A. S. Bishop, H. Bradner, and F. M. Smith, Phys. Rev. 76, 588 A (1949).

   W. H. Barkas, A. S. Bishop, H. Bradner, E. Gardner, and F. M. Smith, Phys. Rev. 78, 886 A (1950).

   W. H. Barkas, E. Gardner, and F. M. Smith, Phys. Rev. 82, 102 L (1950).
4. D. R. Corson and R. B. Brode, Phys. Rev. 53, 773 (1938).

   W. E. Hazen, Phys. Rev. 67, 269 (1945).

   K. M. Crowe, Precision Measurement of the Negative Pion Mass from its Radiative Absorption in Hydrogen, University of California Radiation Laboratory, Report No. UCRL-2050, December, 1952.*
5. W. H. Barkas, Am. Journ. Phys. 20, 5 (1951).
6. H. W. Lewis, Phys. Rev. 85, 20 (1952).
7. W. F. Fry, Phys. Rev. 90, 207 (1953).
8. A. J. Oliver, Measurements of the Effects of Moisture in Nuclear Track Emulsion, University of California Radiation Laboratory Report No. UCRL-2176, April, 1953.
9. F. Bloch, Phys. Rev. 70, 450 (1946).
10. M. Jakobson, A. Schultz and J. Steinberger, Phys. Rev. 81, 895 (1951).
11. T. Eguchi, Phys. Rev. 85, 943 L (1952).
12. H. Morinaga and W. F. Fry, Il Nuovo Cimento 10, 308 (1953).

    D. F. Sherman, Phys. Rev. 90, 469 (1953).
13. J. W. M. DuMond, Phys. Rev. 82, 555 (1951).
14. N. F. Mott, Proc. Roy. Soc. a 124, 425 (1929).

    G. Wentzel, Han. der Phys. 241, 707 (1933).
15. W. H. Barkas, W. Birnbaum and F. M. Smith, Phys. Rev. 91, 765 L (1953).
16. R. T. Birge, Phys. Rev. 40, 213 (1932).

---

*The compatibility of these results with ours indicates a z of unity.

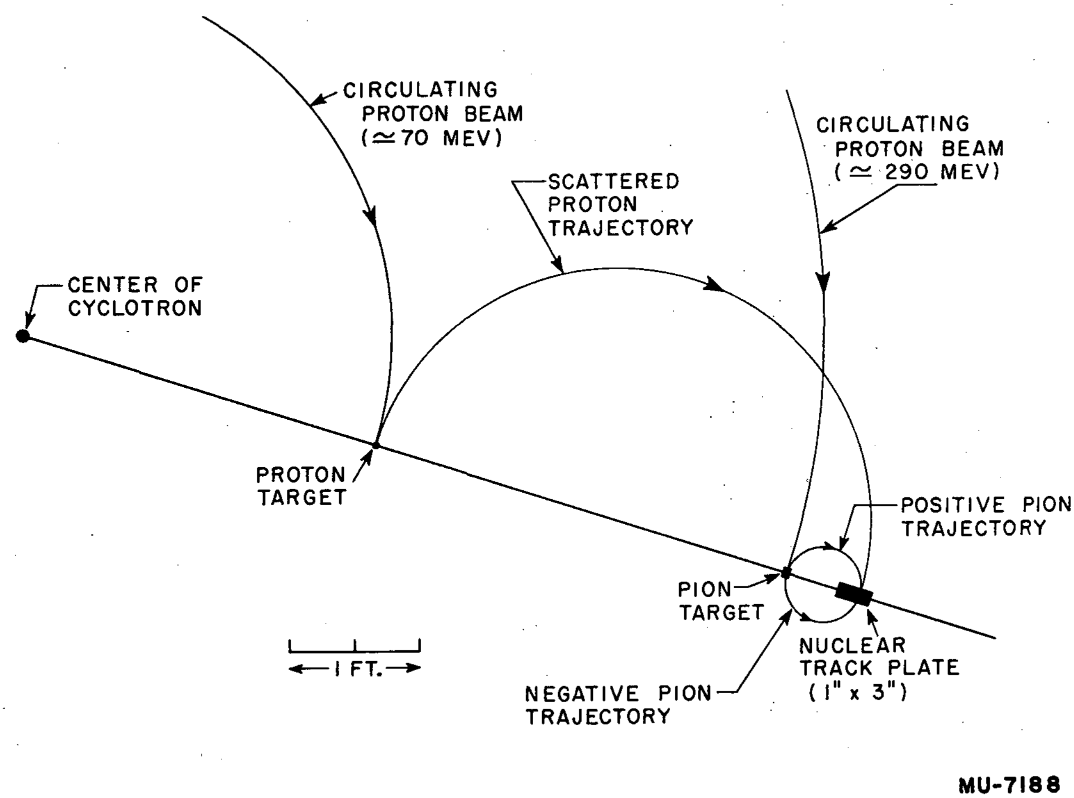

Fig. 1 - Basic plan of the apparatus showing the two targets and the detector plate. The targets were not in place simultaneously during the bombardments. The surface of the emulsion was somewhat below the level of the circulating beam so that the particles entered the emulsion through the "upper" surface with a small angle of dip.

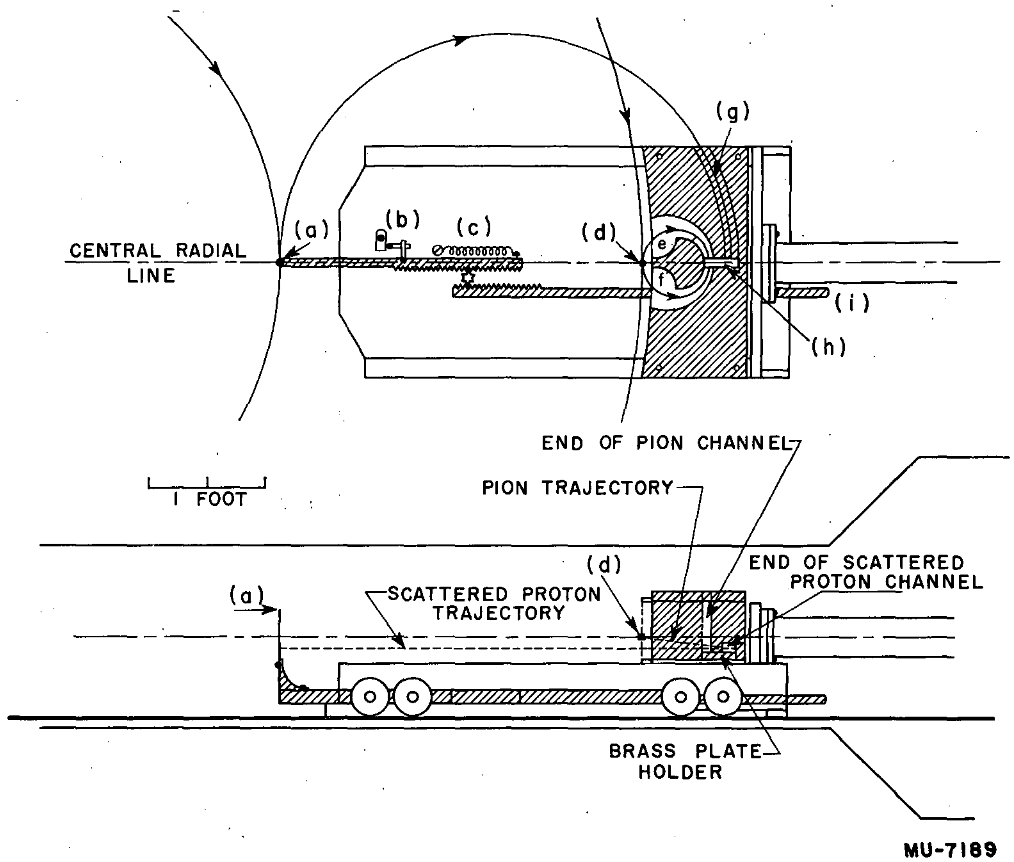

Fig. 2 - Detailed sketches of the top and side view of the apparatus mounted on the probe cart showing:

a. The scattered-proton target.
b. The stop for defining the amount of extension of the proton target.
c. Elastic member which extends the proton target when (i) is not in contact with the lock door.
d. The pion target.
e. The positive-pion channel.
f. The negative-pion channel.
g. The proton channel.
h. Nuclear-track plate on top of the plate holder.
i. The end of the extensible rod that contacts the air-lock door.

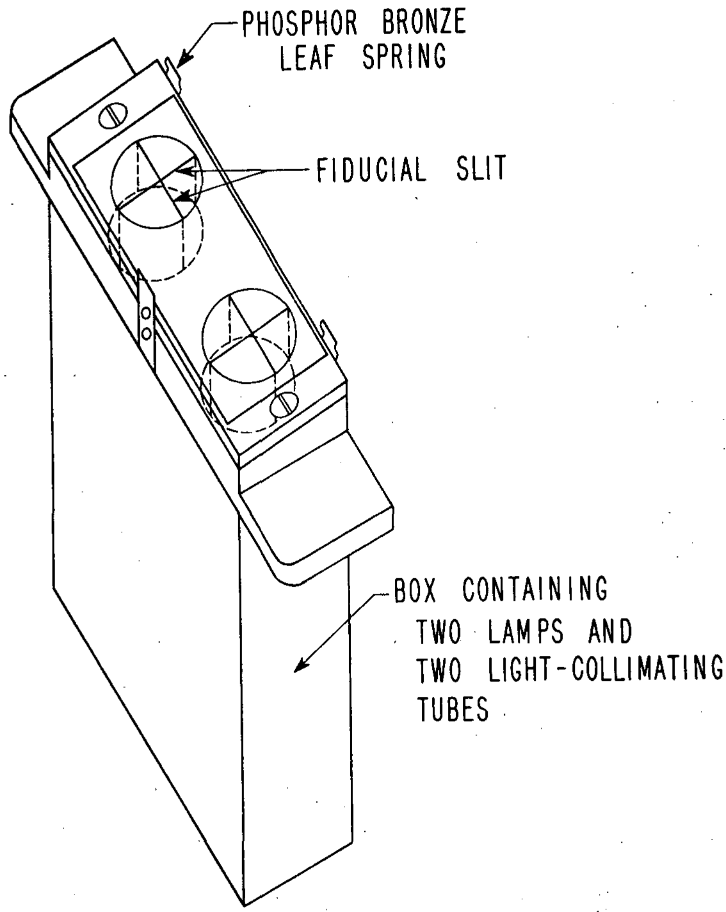

MU-7190

Fig. 3 - Phantom view of the plate holder showing the fiducial slits and the light-bulb container. The 1" x 3" plate is held in position with the emulsion surface up by the leaf springs.

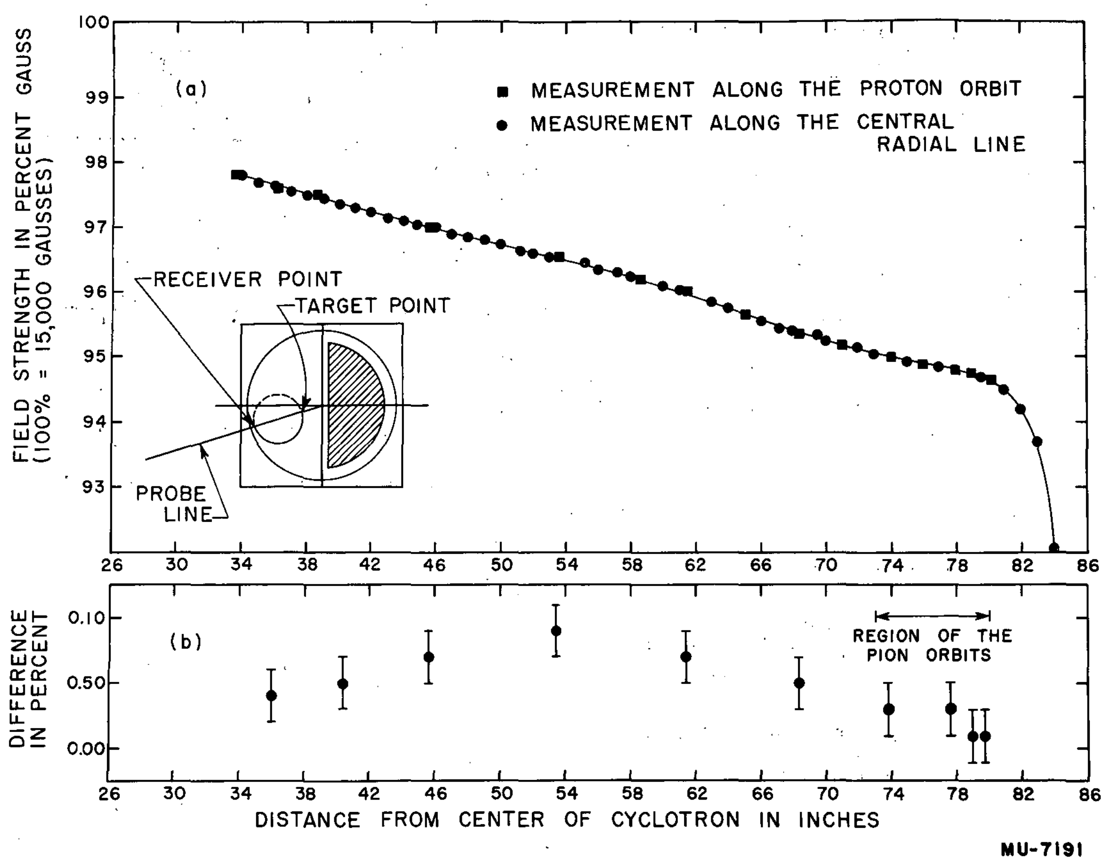

Fig. 4 - (a) Radial variation of the magnetic field strength of the 184-inch magnet as measured along the scattered-proton orbit and along the central radial line.

(b) Radial variation of the difference in field strength between the proton orbit and its mirror image.

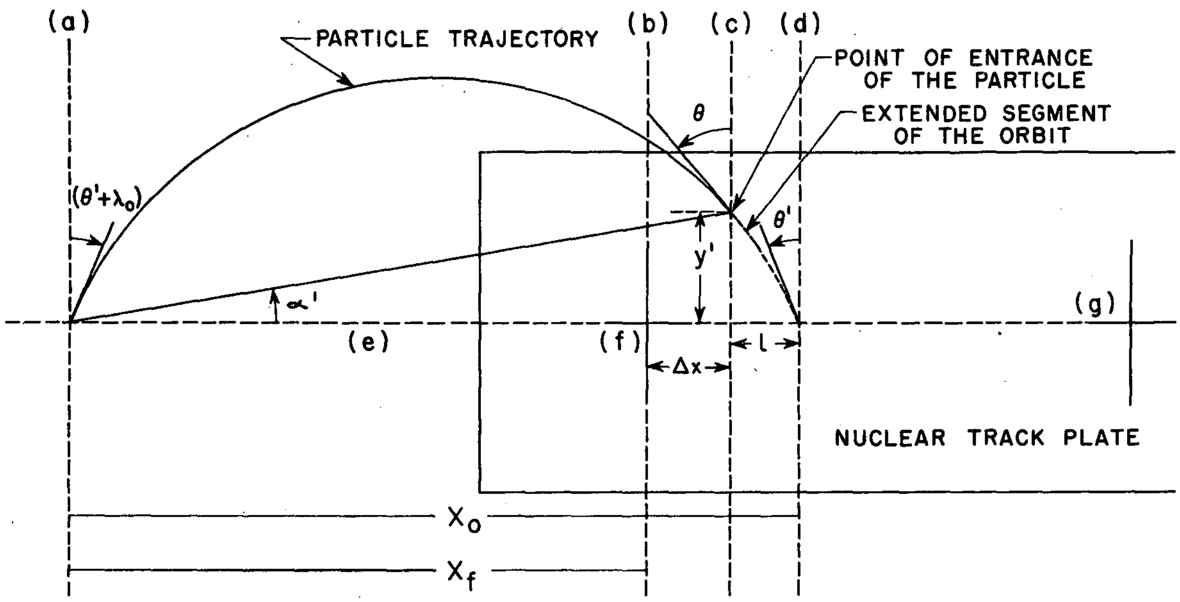

$$l \simeq y' \tan(\theta - \alpha')$$

$$\theta' \simeq (\theta - 2\alpha')$$

$$X_0 \simeq X_f + \Delta x + y' \tan(\theta - \alpha')$$

$$r_1 + X_f = 80 \text{ INCHES}$$

MU-7192

Fig. 5 - Schematic diagram of a particle orbit terminating on the plate showing:

a. The local y axis through the target.
b. The local y axis through the fiducial mark.
c. The local y axis through the entrance point of the particle.
d. The local y axis through the point at which the particle orbit crosses the Central Radial Line.
e. The Central Radial Line (x axis is along this line).
f. The pion fiducial mark.
g. The proton fiducial mark.

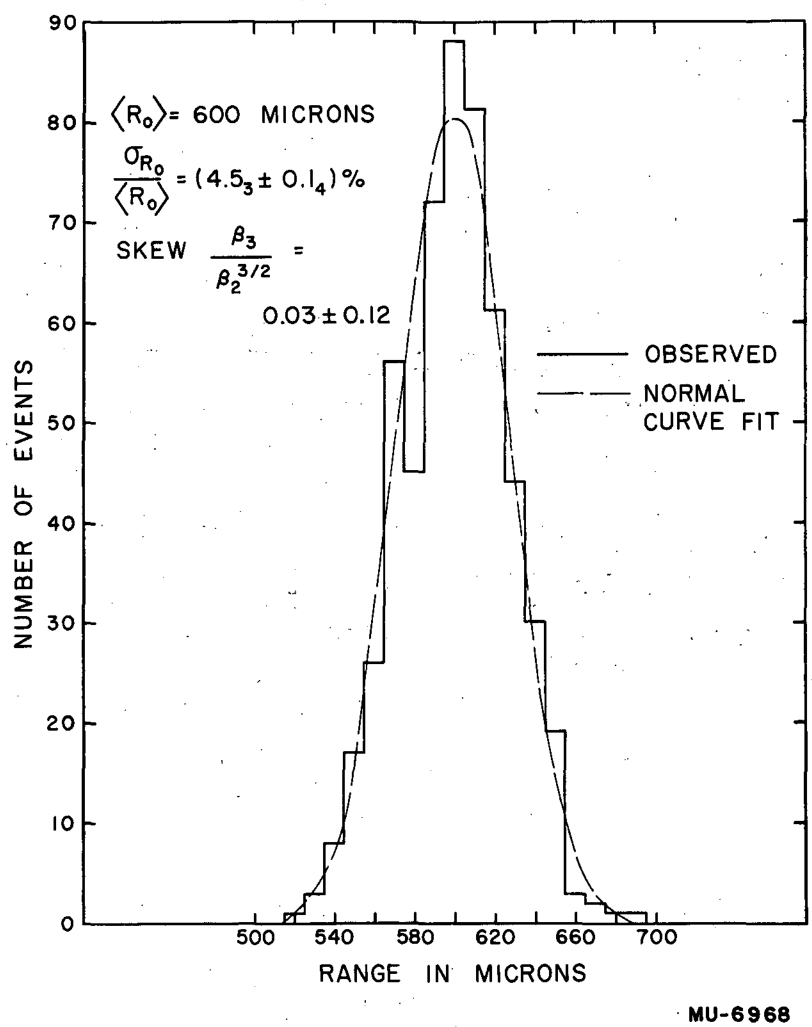

Fig. 6 - Distribution of the ranges of 558 tracks of muons arising from decay at rest of positive pions stopped in the emulsion. The standard deviation is 27 microns.

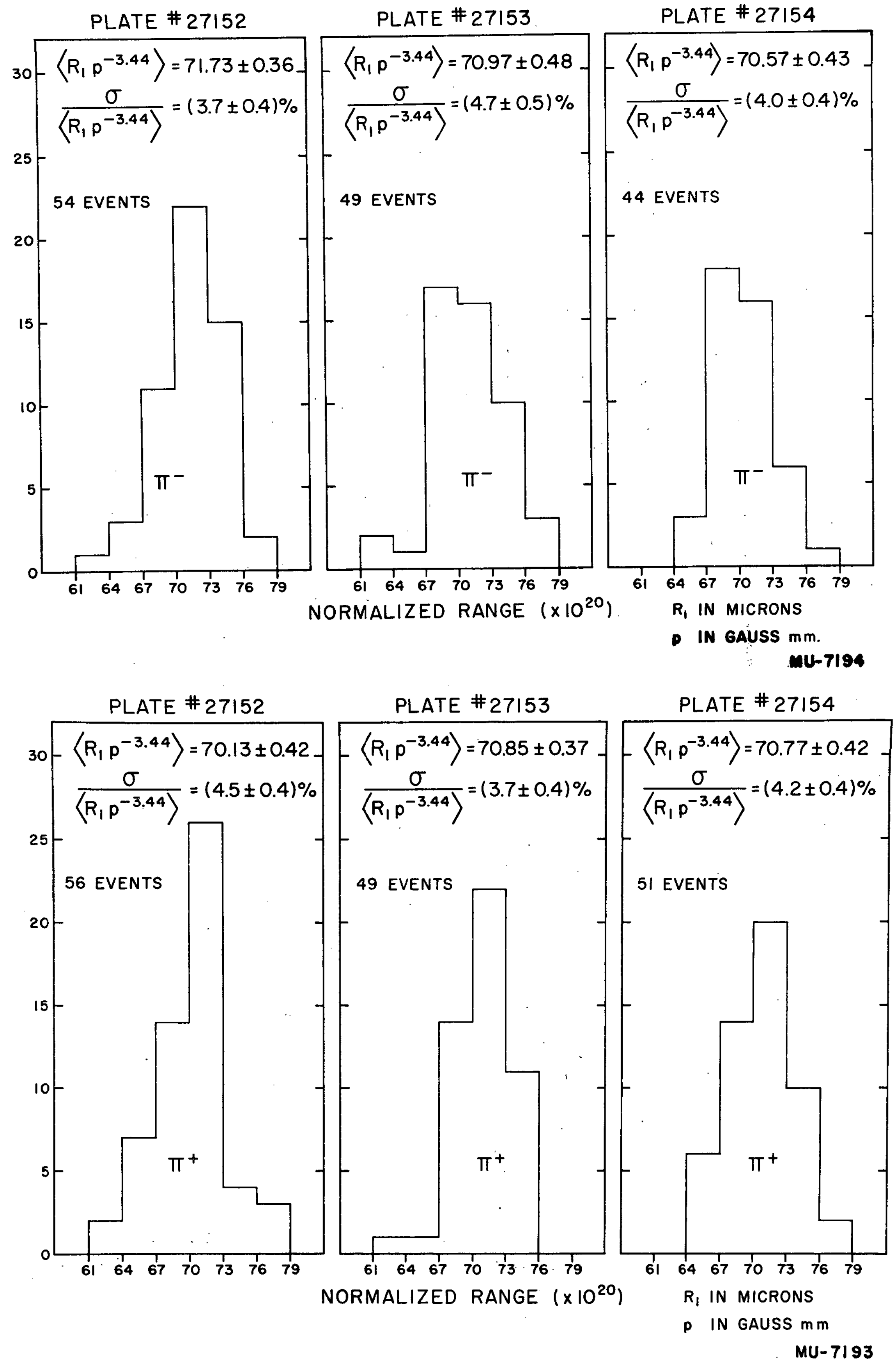

Fig. 7 - Distributions of the normalized ranges of the negative and positive pions in the three plates of part I of the experiment.

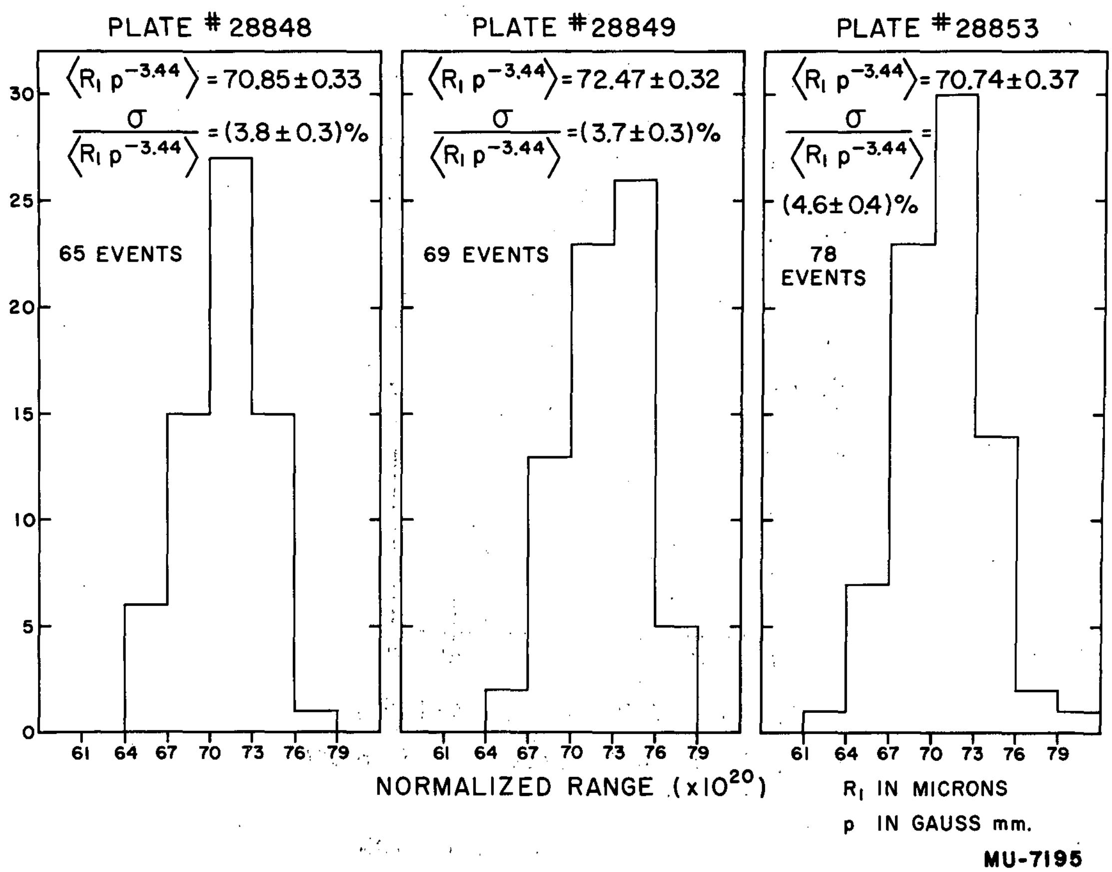

Fig. 8 - Distributions of the normalized ranges of the positive pions in the three plates of part II of the experiment.

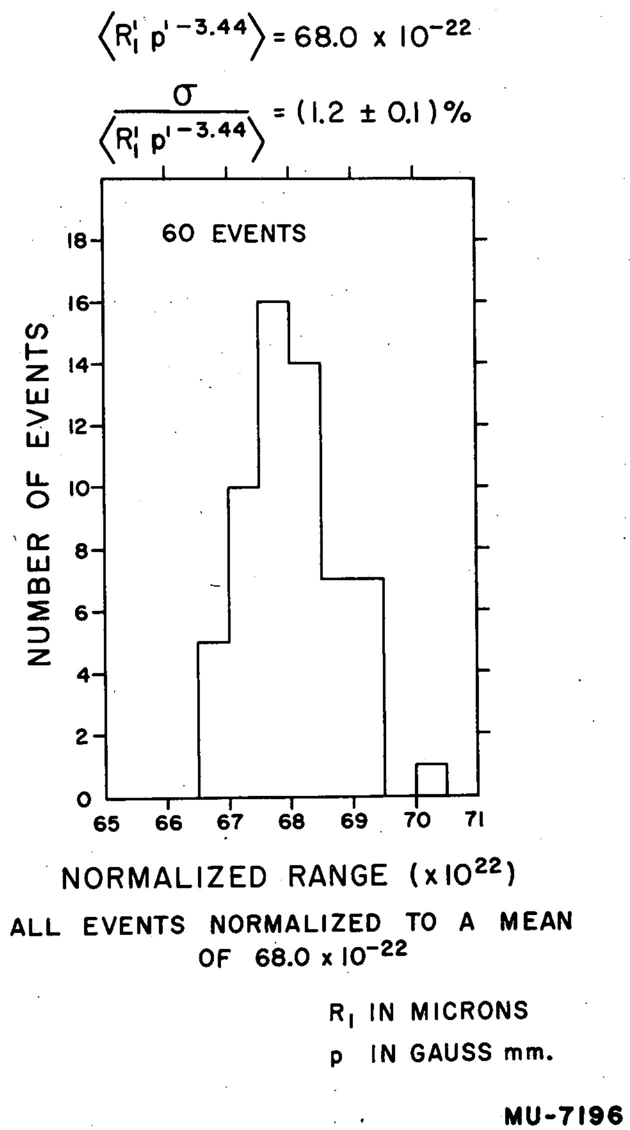

Fig. 9 - **Distribution of the normalized ranges of the protons from** the six plates used in the study. Each of the six distributions has been normalized to a mean of 68.0×10^{-22} comparison.